



# A Novel Steerable Catheter Controlled with a Biohybrid Actuator: A Feasibility Study

Carlotta Salvatori<sup>1,2</sup>, Diego Trucco<sup>1,2</sup>, Ignazio Niosi<sup>1,2</sup>, Leonardo Ricotti<sup>1,2</sup>,  
and Lorenzo Vannozzi<sup>1,2</sup>✉

<sup>1</sup> The BioRobotics Institute, Scuola Superiore Sant'Anna, 56127 Pisa, Italy  
Lorenzo.vannozzi@santannapisa.it

<sup>2</sup> Department of Excellence in Robotics & AI, Scuola Superiore Sant'Anna, 56127 Pisa, Italy

**Abstract.** Targeted therapies allow increasing the efficacy of treatments for several diseases, including cancer. The release of drugs or chemicals directly in the site of interest will be beneficial for maximizing the therapy and minimize side effects.

Here, we report the concept and a preliminary analysis of an innovative intravascular steerable catheter guided by an on-board biohybrid actuator, aiming to release drugs into deep and tortuous regions within the cardiovascular systems. The catheter performance has been estimated through analytical and numerical analyses, varying catheter diameter, wall thickness, and actuator force. Results show how larger catheter deflections can be obtained with a smaller outer diameter and decreasing wall thickness. Besides, improved outcomes can be achieved by applying the biohybrid actuator distant from the catheter tip extremity and maximizing the magnitude of the applied forces. Despite the need to further improve the performance of this concept (e.g., by decreasing material stiffness), these preliminary results show great promise in view of future experimentation of such kind of actuation to drive microcatheters through the cardiovascular network.

**Keywords:** catheter · biohybrid actuator · drug release · living machine

## 1 Introduction

Cancer is a worldwide disease consisting of uncontrolled growth of cells, which can even go beyond their usual boundaries to invade nearby parts of the body. The American Cancer Society reports that, for solid cancers, more than 1.8 million cases are expected in 2023 [1].

The current gold standards for cancer therapy depend on the cancer location. They include surgical removal, radiation therapy, and chemotherapy [2]. In particular, chemotherapy aims to stop the growth of cancer cells, either by killing the cells or preventing their division. Chemotherapy is typically given through injection or infusion by central venous catheters or orally taken as pills. The drugs used in chemotherapy, such as cisplatin, are meant to attack cells that proliferate quickly, including cancer cells, and those found in the blood and hair bulbs. Thus, systemic administration may result in many undesirable effects on the patient, such as hair loss, nausea, and vomit.

© The Author(s) 2023

F. Meder et al. (Eds.): Living Machines 2023, LNAI 14158, pp. 378–393, 2023.

[https://doi.org/10.1007/978-3-031-39504-8\\_26](https://doi.org/10.1007/978-3-031-39504-8_26)

To mitigate such side effects, a desirable approach would be to target the tumor directly navigating the arteries through a catheterization, allowing for the delivery of the medication in the target area. A recent example of a therapy developed to treat a specific organ, such as the liver, is the hepatic arterial infusion therapy (HAI) [3]. Hepatocellular carcinoma is one of the most common cancers worldwide and, nowadays, the only curative treatment is surgery, liver transplantation, and percutaneous ablation. HAI therapy consists of a surgical procedure to implant a wireless pump at the level of the abdomen, connected to a catheter that supplies a drug directly to the hepatic artery. Thus, the therapy is administered only to the liver over a period of time and cycles. The main limitations of HAI are the need for surgery (some patients cannot undergo surgery because of their impaired health status) and the risks associated with surgery complications [4, 5].

Understanding the anatomy of the arteries supplying the cancer is crucial for improving the treatment by catheterization. However, conventional catheters may not effectively reach the target due to the high degree of tortuosity in the artery network, which becomes increasingly complex toward the target organ and organ region. Therefore, there are ongoing studies to develop steerable catheters with an orientable tip, which can enhance their ability to access deeper and tortuous regions. Steerable catheters can be categorized based on their actuation method, which either generates force at the tip or transmits force to the tip. The former can be further classified into electric, thermal, and magnetic actuation, while the latter can be subdivided into hydraulic actuation and mechanical cable actuation [6]. Each category has its own set of limitations. In the case of electrical actuation, an electrical current is supplied to the actuator to generate a bending force and movement at the distal tip. Such an approach has inherent restrictions on the degree of bending movement that can be obtained. Additionally, there are concerns about the safety of the materials used in an aqueous environment, such as the bloodstream in which the catheter is immersed, due to the intensity of the current needed to actuate the catheter. Instead, thermal actuation exploits shape memory alloys, thus encountering problems in fabrication procedures, overheating hazards, and temperature dependence.

The principle behind magnetic actuation is typically the manipulation of a magnetic field, applied to the distal end of the catheter containing magnetic-responsive elements. Kim *et al.* recently conducted an interesting study in which they developed a 500  $\mu\text{m}$  diameter steerable catheter, magnetically controlled thanks to the presence of NdFeB nanoparticles dispersed in the soft polymer matrix of the body, composed of silicone (polydimethylsiloxane, PDMS) or thermoplastic polyurethane [7]. However, the limitations associated with magnetic actuation are mainly due to the cost and complexity of the external field-generating system to be used in a surgical scenario.

Regarding the approaches developed to transmit force to the tip, the hydraulic actuation takes advantage of channels running through the entire length of the catheter, through which a fluid or air is injected to generate pressure capable of steering the catheter. Recently, Goseph *et al.* developed a tip with hydraulic actuation, characterized by an outer diameter of 900  $\mu\text{m}$  and four channels of 50  $\mu\text{m}$  diameter filled with saline solution [8]. However, drawbacks include limitations inherent in the catheter design, the need for manual manipulation of the proximal tip movements, the extended length of the catheter, and the requirement for pressures as high as 4 Bar. Catheters are usually

steered by cable-driven systems controlled by mechanical wires that are driven from their base, and require the passage through the entire length of the catheter [9]. Many commercial solutions have been developed with this technology. For example, a steerable microcatheter with cable actuation and remote control via a steering dial placed proximally on the grip was developed in 2014. The catheter, characterized by a diameter of 900  $\mu\text{m}$ , was connected to the steering dial by two wires inserted through lumens in the wall, and the tip could be manipulated by applying tension to the cables [10]. Therefore, they also have limitations in design due to the cables themselves, difficulties in control by the physician, and they can be impeded by twisting and instability that can lead to undesired tip movements.

However, remotely controlling miniaturized catheters intravascularly to deliver drugs to difficult-to-access regions remains a challenge. In this paper, we propose a novel approach to drive a steerable catheter, based on a biohybrid actuator integrated on-board, in the catheter tip (Fig. 1).

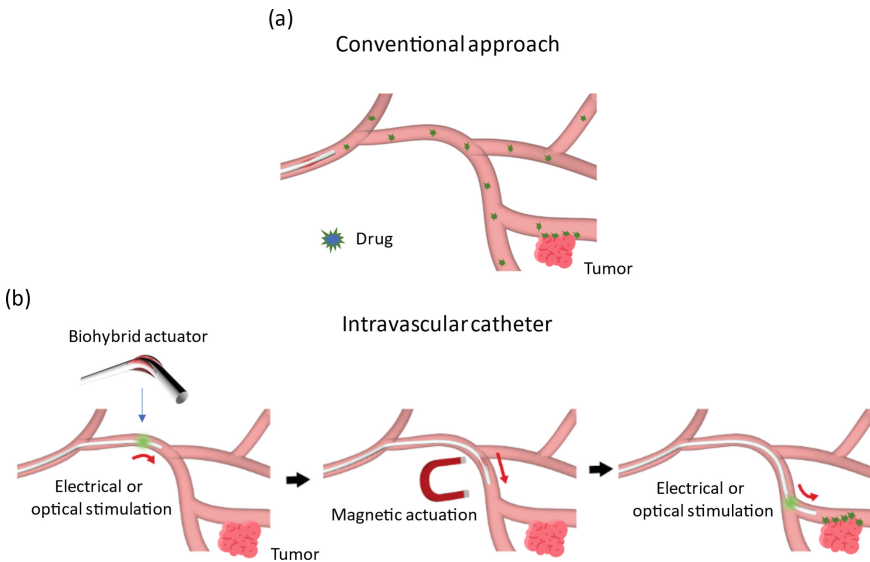


**Fig. 1.** Comparison between a conventional catheter-assisted drug release and the proposed biohybrid catheter concept, in which the scalability of the biohybrid motors may assist the achievement of a narrower district to deliver a chemotherapeutic drug. (a) Traditional catheters allow to deliver chemotherapeutic drugs relatively far from the cancer location; consequently, a considerable amount of drug is delivered to healthy tissues, with side effects. (b) The newly proposed biohybrid catheter combines magnetic steering and bending of the tip exploiting the force produced by a biohybrid actuator integrated on-board (that can be triggered on-demand by the user through electrical stimuli or optical ones, in the case of optogenetically-modified cells). This allows the release of chemotherapeutic drugs in a highly targeted way, minimizing the side effects.

Biohybrid actuators integrate living organisms, such as contractile muscle cells, with artificially engineered structures, to develop machines with unconventional functionalities. Natural muscle is a soft biological actuator derived from millions of years

of evolution, featured by performance invariance with scalability, outstanding driving capability, compliance, and additional functions such as self-healing. Biohybrid actuators offer the advantage of maintaining contractile performance and high actuation efficiency, particularly when scaled down from centimeter to micrometer sizes [11–13]. Moreover, muscle cell-based actuators can generate a significant force on the milli and micrometer-scale, higher than 100  $\mu\text{N}$  up to mN [14, 15]. Also, they exploit their ability to convert chemical energy from their environment into mechanical energy, eliminating the need for external power sources, which can be hardly scaled down in size.

In this work, we propose the innovative concept of a steerable catheter tip actuated by a muscle cell-based actuator. We explored the design of such a concept by envisioning the fabrication of a soft catheter tip made of silicone, which incorporates a biohybrid actuator based on skeletal muscle cells that can deflect the tip. A preliminary analysis of the physical and geometrical parameters of the catheter tip is reported, putting them in relationship with the estimated catheter deflection generated by the force produced with the biohybrid actuator. A numerical analysis has been performed to investigate the bending dynamic of the tip by varying the biohybrid actuator configuration, with the aim to maximize the tip deflection.

## 2 Materials and Methods

### 2.1 Material Selection, Preparation and Mechanical Evaluation

For the design of the catheter tip, we considered different types of soft silicones, such as PDMS (Sylgard 184 silicon elastomer kit, Dow), Ecoflex 00-10 (Smooth-On), and different ratios to tune their mechanical properties. Silicones were chosen because they are tunable and soft materials that can be modified to host cell cultures on their surface. Indeed, cell cultures on silicones can be promoted by activating their surface with a plasma treatment, which can favor protein coatings, thus an excellent cell adhesion and growth [16]. PDMS is biocompatible and can be functionalized through plasma [17]. On the other hand, Ecoflex 00–10 cannot be tailored easily through plasma-assisted modifications, but they have a smaller elastic modulus and larger viscosity [18, 19].

PDMS was tested at the monomer/curing agent ratio of 10:1 and 20:1, while Ecoflex 00-10 was prepared according to the manufacturer's instructions. PDMS was mixed with Ecoflex 00–10 by preparing each silicone separately to the desired ratio. After mixing for 2 min, the solution was degassed using a centrifuge, set at 1300 RCF for 5 min.

Tensile tests were performed using an INSTRON machine (model 2444, load cell: 1 kN, Instron, Norwood, MA, USA), with specimens obtained through a mold designed following ASTM-D638, applying a tensile speed of 10 mm/min. The Young's modulus was derived from the slope of the first 10% of the stress-strain graph.

### 2.2 Estimation of the Catheter Flexural Rigidity

The catheter's geometrical and physical properties influence the deflection of the catheter [20]. These parameters can be summarized in the flexural rigidity ( $F_l$ ), which can be calculated as follow:

$$F_l = E * I_0 \quad (1)$$

where  $E$  is the Young’s modulus and  $I_0$  denotes the moment of inertia of a hollow structure:

$$I_0 = \frac{\pi(D^4 - d^4)}{64} \tag{2}$$

where  $D$  is the external diameter and  $d$  is the internal diameter.

Another encountered phenomenon when placing a catheter is kinking, which refers to the potential obstruction that may occur when the radius of curvature becomes smaller than a critical value ( $R_{critical}$ ). This  $R_{critical}$  can be defined as:

$$R_{critical} = \frac{(1 - \nu^2) * R^2}{K * t} \tag{3}$$

where  $R$  is the external radius of the catheter,  $t$  is the wall thickness,  $\nu$  is the Poisson’s ratio (set to 0.48 [21]) and  $K$  is a constant (theoretically = 0.99; experimentally 0.72–1.14) [22].

**2.3 Expected Deflection by Euler-Bernoulli Beam’s Theory**

Euler-Bernoulli’s beam theory has been used to calculate catheter deflection, assuming a linear mechanical behaviour of the material at small deformations [23, 24]. Considering the force ( $F$ ) exerted by the biohybrid actuator, the catheter will be subject to a moment  $M$  equal to:

$$M = F * \frac{D}{2} \tag{4}$$

Then, for the Euler-Bernoulli’s beam theory, the deflection induced by the biohybrid actuator can be calculated as follows:

$$\delta = \frac{M * x1^2}{2 * E * I_0} \tag{5}$$

where  $x1$  is the length of the biohybrid actuator (Fig. 2).

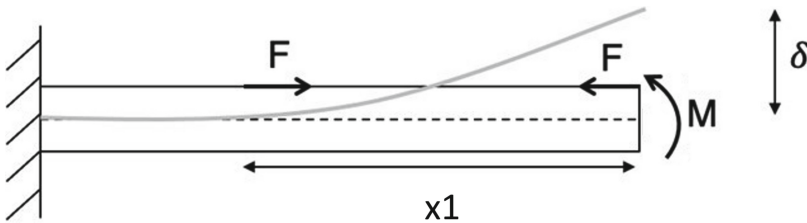


**Fig. 2.** Representation of applied forces, torque, and deflection generated on a beam, used as a model of the catheter tip.

## 2.4 Numerical Analysis of the Catheter Bending

Structural finite element model (FEM) simulations were performed using COMSOL Multiphysics v5.6 (COMSOL Inc., Sweden) to support the analytical modelling of catheter deflection. The module “solid mechanical” was used, and the mesh was set to normal (physics-controlled mesh, number of elements: 6065, minimum elements quality: 0.2046) after the evaluation of the mesh convergence. We defined a model consisting of a hollow cylinder with an outer radius of 1 mm ( $D = 2$  mm), an inner radius of 0.75 mm ( $d = 1.5$  mm) and a catheter tip length ( $lc$ ) of 15 mm. Two axial load points were applied to the outer wall of the catheter ( $p1$  and  $p2$ ), with the same magnitude and opposite direction, simulating the biohybrid actuator contraction behavior as a strip of muscle tissue, with a length defined as  $x1$  (Fig. 3).

The geometrical parameters of the biohybrid actuator, such as its positioning over the catheter wall, length, and the force magnitude applied, were varied in the analyses.

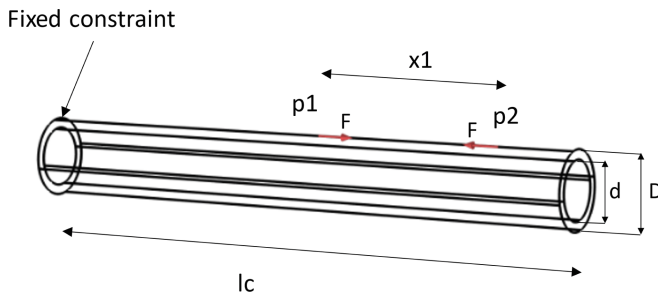


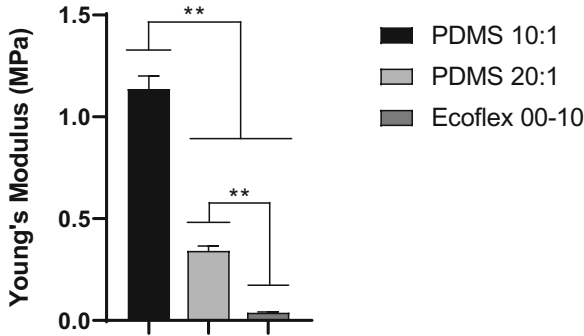
**Fig. 3.** Depiction of the model implemented in COMSOL, and of the variables considered in the analysis.

## 3 Results and Discussion

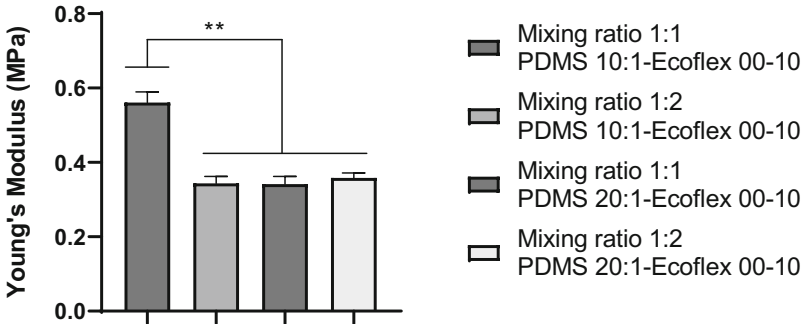
### 3.1 Mechanical Characterization

Figure 4 and Fig. 5 show the mechanical analysis results for PDMS 1:10, PDMS 1:20 Ecoflex 00–10 and mixes between PDMS and Ecoflex 00–10.

Among the materials examined, PDMS 10:1 was the stiffest one, Ecoflex 00–10 kept the lowest elastic modulus, whereas PDMS 20:1 displayed a medium elastic modulus. Then, we tried to mix PDMS 20:1 and Ecoflex to decrease the material Young’s modulus to maintain the PDMS chemistry as a highly tailorable one for cell cultures. As can be seen in the Fig. 5, we noticed a saturation in Young’s modulus variation, down to an average value close to 0.34 MPa for the mix between PDMS 1:10 and Ecoflex 00–10 in a ratio 1:2, and PDMS 1:20 and Ecoflex for both ratios (1:1 and 1:2). We kept this value as a reference for the following analyses.



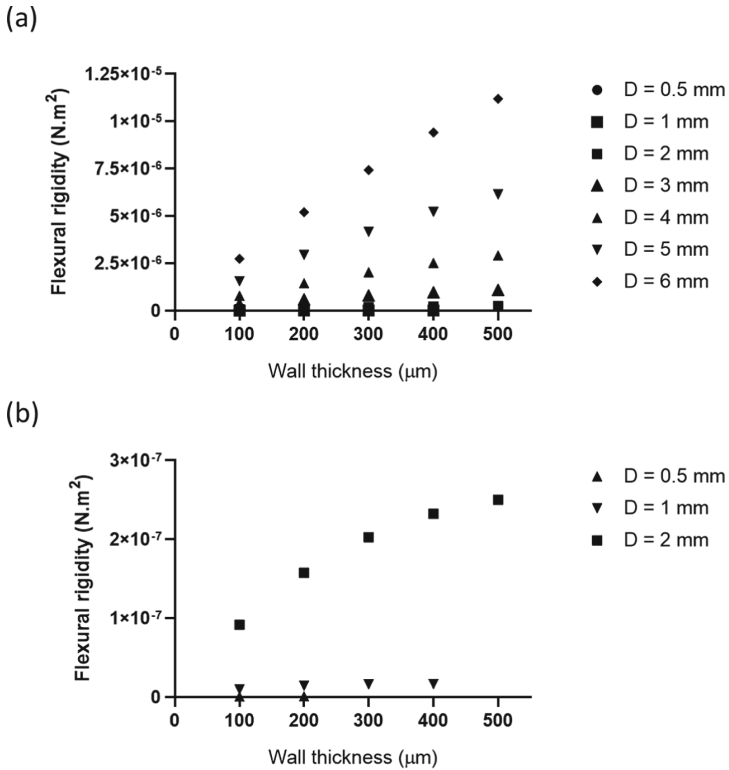
**Fig. 4.** Young's moduli of the silicones considered in this study. Data underwent ANOVA test and Tukey's post-hoc comparison, \* =  $p < 0.05$ , \*\* =  $p < 0.01$ . N = 5.



**Fig. 5.** Young's moduli of different combinations of PDMS and Ecoflex 00–10. Data underwent ANOVA test and Tukey's post-hoc comparison, \* =  $p < 0.05$ , \*\* =  $p < 0.01$ . N = 5.

### 3.2 Flexural Rigidity, and the Influence of the Physical and Geometrical Parameters

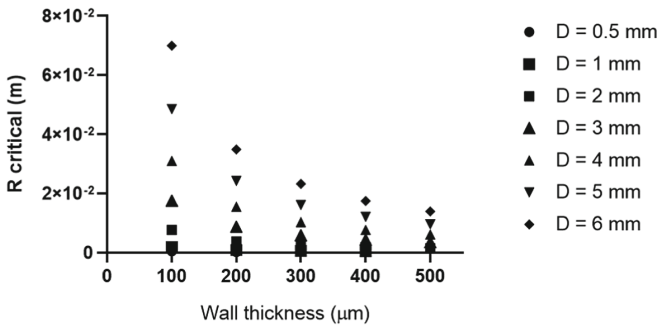
In Fig. 6a and Fig. 6b, it is noticeable that as the outer diameter (from 0.5 to 6 mm) and the wall thickness (from 100 to 500  $\mu\text{m}$ ) increase, the catheter flexural rigidity also considerably increases, based on the analytical model described in Sect. 2.3. Flexural rigidity represents the tendency for the catheter to mechanically oppose when a moment is applied, and it is proportional to the stress that is applied on the vessel wall by the catheter itself. Therefore, a low value of flexural rigidity is desirable to maximize the catheter deflection. These results also suggested that catheters with smaller diameters will tend to oppose a lower resistance to the torque applied by the biohybrid actuator.



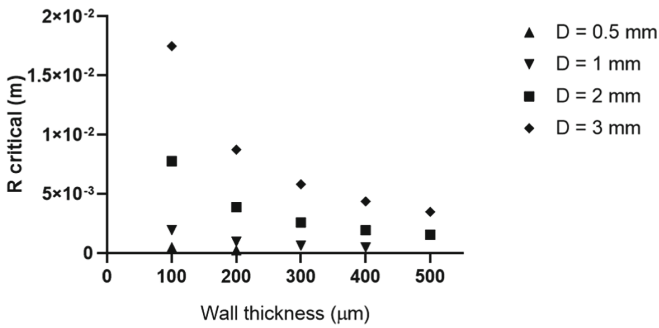
**Fig. 6.** (a) Flexural rigidity over the outer diameter and wall thickness variation. (b) Magnification for the cases  $D = 0.5 \text{ mm}$ ,  $D = 1 \text{ mm}$ , and  $D = 2 \text{ mm}$ .

Figure 7a and Fig. 7b show the critical radius to not incur in kinking phenomena. Here, it is noticeable how the wall thickness influences the  $R_{critical}$ , and how this value increases while decreasing the catheter size. Typical values of flexural rigidity of catheters range from 1 to  $50 \cdot 10^{-4} \text{ N} \cdot \text{m}^2$ , mainly due to the stiffness of the material used to fabricate the catheter (higher than silicones) [25]. The possible occurrence of kinking phenomena is an important parameter of catheters to take into account because of the need to avoid occlusions during steering. The final dimensioning of the catheter should be also driven by avoiding the achievement of such curvatures.

(a)



(b)



**Fig. 7.** (a)  $R_{critical}$  over the outer diameter and wall thickness variation. (b) Magnification for the cases  $D = 0.5$  mm,  $D = 1$  mm,  $D = 2$  mm, and  $D = 3$  mm.

### 3.3 Estimation of the Catheter Deflection/Curvature

The catheter deflection has been analytically estimated by varying specific geometrical and physical parameters, such as the diameter, wall thickness and force applied by the actuator. It is possible to observe from Fig. 8a and Fig. 8b a drastic decrease in deflection as the outer diameter increases from 0.5 to 6 mm. When a catheter has a small diameter (e.g.,  $D = 0.5$  mm), it has a lower inertia, and can achieve greater deflection values than larger-diameter systems.

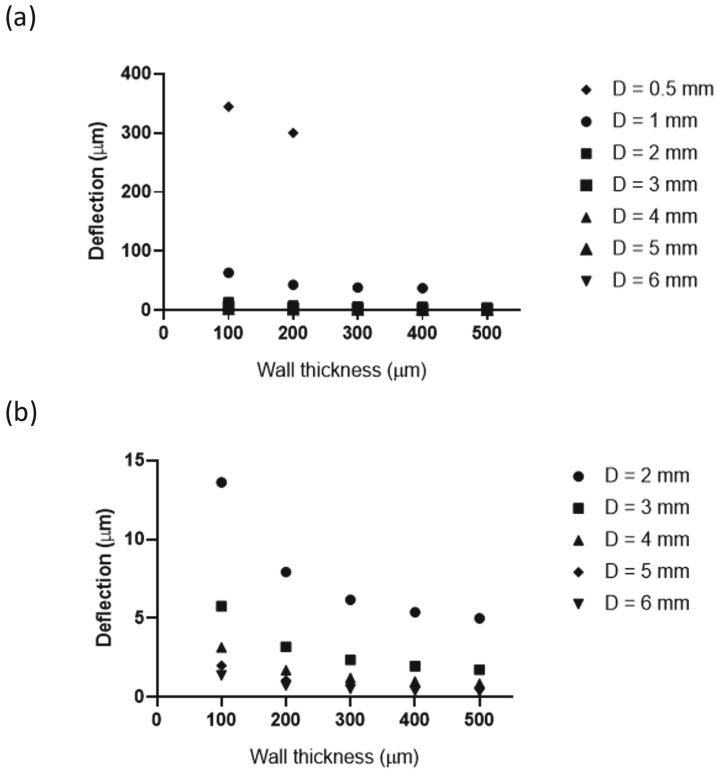


**Fig. 8.** (a) Analysis of the catheter deflection over the outer diameter and wall thickness variation. (b) Magnification for the cases  $D = 2$  mm,  $D = 3$  mm,  $D = 4$  mm,  $D = 5$  mm, and  $D = 6$  mm.

We also analyzed the influence of the force for a specific case ( $D = 2$  mm). That is a suitable diameter to move forward to the left or right branches of the hepatic artery [26]. As shown in Fig. 9, increasing the biohybrid actuator force from  $100 \mu\text{N}$  to  $500 \mu\text{N}$  [12], the expected deflection increased proportionally up to about  $70 \mu\text{m}$  from  $15 \mu\text{m}$ .

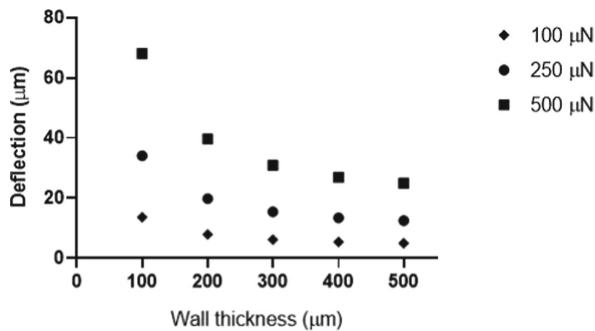
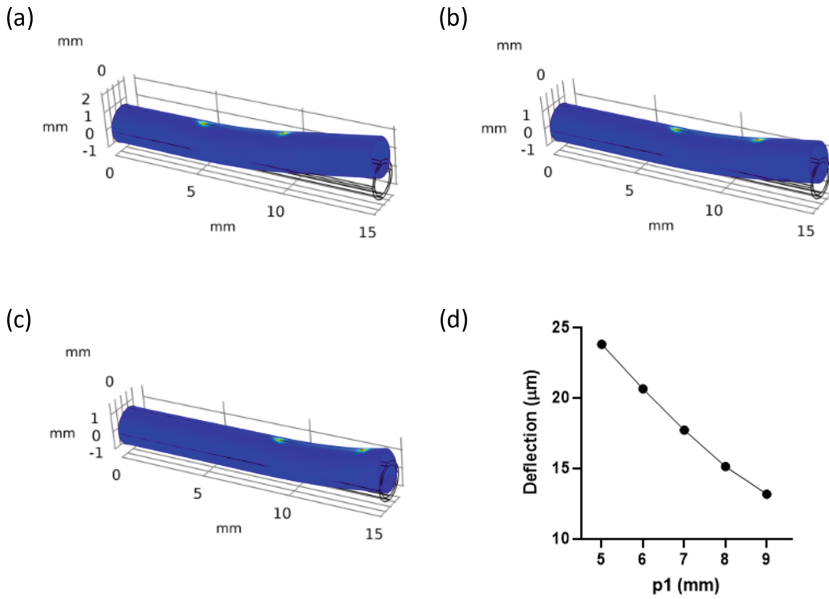


**Fig. 9.** Analysis of the catheter deflection over the wall thickness variation for the case  $D = 2$  mm.

### 3.4 Simulation of the Catheter Deflection

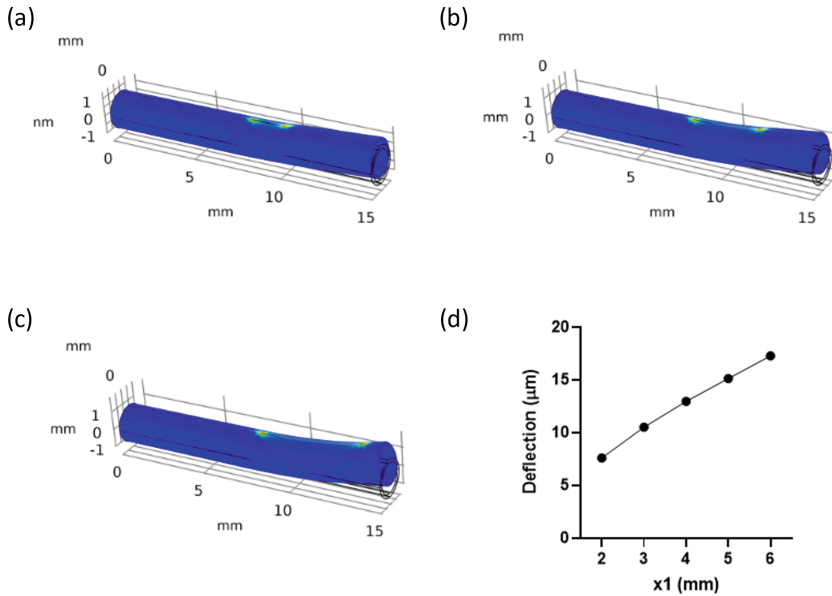
For the numerical analysis, the deflection variation was analyzed by varying the spatial configuration of the biohybrid actuator (position and length) and the force magnitude.

Figure 10 reports that the deflection decreases with the increase of the distance between the application of the first load point and the fixed constraint ( $p1$ ).



**Fig. 10.** Representation of results obtained by varying  $p1$ : (a) 5 mm, (b) 7 mm, and (c) 9 mm. Other parameters set are:  $D = 2$  mm,  $t = 200$   $\mu\text{m}$ ,  $l_c = 15$  mm,  $E = 0.34$  MPa,  $x_1 = 5$  mm,  $F = 100$   $\mu\text{N}$ . Scale factor 50. (d) Deflection estimated by varying the distance  $p1$ .

The deflection was higher at the lowest value of  $p1$  (23.8  $\mu\text{m}$ ), and decreased up to 13.2  $\mu\text{m}$  ( $p1 = 9$  mm). On the other hand, Fig. 11 shows the variation obtained by varying the distance between the points of application of the forces ( $x1$ ), so essentially varying the biohybrid actuator length, keeping  $p1$  fixed at 8 mm.



**Fig. 11.** Representation of results obtained by varying the length of the biohybrid actuator ( $x1$ ): (a) 2 mm, (b) 4 mm, and (c) 6 mm. Other parameters set are:  $D = 2$  mm,  $t = 200$   $\mu$ m,  $l_c = 15$  mm,  $E = 0.34$  MPa,  $p1 = 8$  mm,  $F = 100$   $\mu$ N. Scale factor 50. (d) Deflection estimated by varying the biohybrid actuator length ( $x1$ ).

In this case, the deflection increases from  $7.6$   $\mu$ m ( $x1 = 2$  mm) up to  $17.3$   $\mu$ m ( $x1 = 6$  mm). As the distance between the points at which the forces are applied increases, there is a higher deflection of the catheter. This means that the length of the biohybrid actuator is relevant in improving the catheter deflection. Then, another important parameter that can help in maximizing the catheter deflection is the force applied by the biohybrid actuator. In Fig. 12, a variation of the force applied was investigated.

Here, the deflection increases proportionally to the applied force, from  $15.7$   $\mu$ m ( $F = 100$   $\mu$ N) up to  $75.7$   $\mu$ m ( $F = 500$   $\mu$ N). These simulations foresee the analysis of the forces applied on the outer surface of the catheter tip. In the case of forces applied in the inner wall of the catheter (e.g., biohybrid actuator placed internally), the expected deflection will be lower because of the generation of a torque with a lower magnitude due to the lower arm.

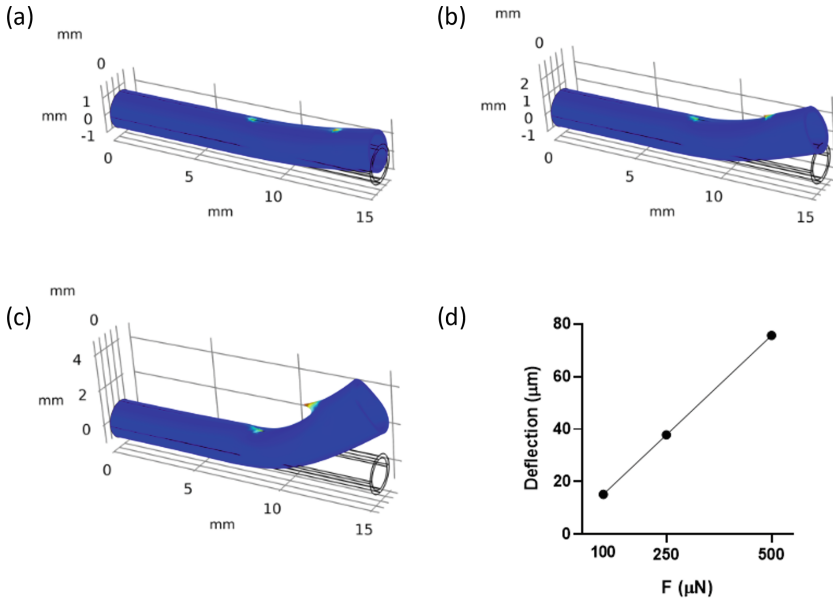


**Fig. 12.** Representation of results obtained by varying  $F$ : (a)  $100 \mu\text{N}$ , (b)  $250 \mu\text{N}$ , and (c)  $500 \mu\text{N}$ . Other parameters set are:  $D = 2 \text{ mm}$ ,  $t = 200 \mu\text{m}$ ,  $l_c = 15 \text{ mm}$ ,  $E = 0.34 \text{ MPa}$ ,  $p_1 = 8 \text{ mm}$  and  $x_1 = 5 \text{ mm}$ . Scale factor 50. (d) Deflection estimated by varying the distance  $F$ .

Finally, an investigation of the parameters providing the highest deflection for each case ( $p_1 = 5 \text{ mm}$ ,  $x_1 = 6 \text{ mm}$ ,  $F = 500 \mu\text{N}$ ) was performed to analyze the performance of the optimized configuration among the cases analyzed (Fig. 13). It can be observed that the deflection achieved a considerably higher value ( $133.4 \mu\text{m}$ ) than the previous simulations, almost doubling the outcome of the most performing parameter ( $F$ ).

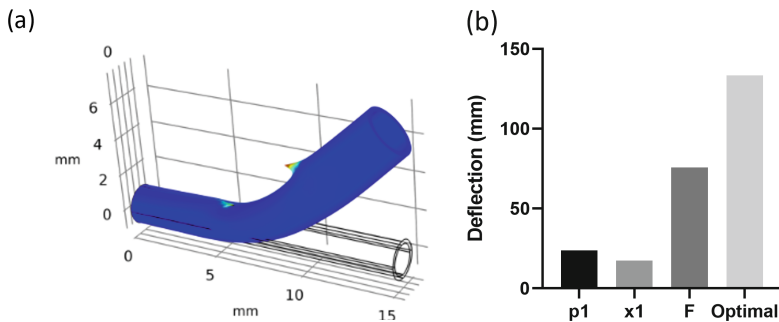


**Fig. 13.** Representation of the catheter bending by setting:  $D = 2 \text{ mm}$ ,  $t = 200 \mu\text{m}$ ,  $l_c = 15 \text{ mm}$ ,  $E = 0.34 \text{ MPa}$ ,  $p_1 = 8 \text{ mm}$ ,  $x_1 = 5 \text{ mm}$  and  $F = 500 \mu\text{N}$ . Scale factor 50. (d) Comparison of the deflections estimated with the previous simulations.

This result demonstrates the need of playing with multiple parameters to improve the catheter deflection, and maximize the performance in view of a steerable catheter controlled with a biohybrid actuator.

## 4 Conclusions

This work reports the concept and preliminary considerations for the design of a steerable catheter actuated by a biohybrid actuator integrated on its tip. Analytical and numerical models were used to estimate the degree of catheter deflection by varying the catheter size, the force exerted by the biohybrid actuator, and its spatial configuration, considering some soft silicones that have been characterized for this application. Future efforts will be also directed to optimize the material properties to manufacture a softer catheter, more compliant to the torque generated by the actuator. Different microfabrication technologies will be explored, including molding, additive manufacturing, self-assembly techniques, and dip coating, by carefully assessing the strengths and limitations of each technology. Then, future work will regard the integration of a flexible electronic platform to facilitate the electrical stimulation required for the muscle cells [27]. Future evolutions may also include light-responsive cells (e.g., subjected to optogenetic modifications [28], or treated with azobenzenes [29]) to make the catheter tip bendable through light pulses transmitted through the catheter structure (that should act as an optical fiber).

**Acknowledgments.** This project has received funding from the European Union's Horizon Europe research and innovation program under grant agreement No. 101070328 (BioMeld project).

## References

1. American Cancer Society. <https://www.cancer.org/research/cancer-facts-statistics/all-cancer-facts-figures/2023-cancer-facts-figures.html>. Accessed 03 Apr 2023
2. Zugazagoitia, J., Guedes, C., Ponce, S., Ferrer, I., Molina-Pinelo, S., Paz-Ares, L.: Current challenges in cancer treatment. *Clin. Ther.* **38**(7), 1551–1566 (2016)
3. Obi, S., Sato, S., Kawai, T.: Current status of hepatic arterial infusion chemotherapy. *Liver Cancer* **4**(3), 188–199 (2015)
4. OHSU Knight Cancer Institute. <https://www.ohsu.edu/knight-cancer-institute/hepatic-arterial-infusion-hai>. Accessed 29 May 2023
5. Song, M.J.: Hepatic artery infusion chemotherapy for advanced hepatocellular carcinoma. *World J. Gastroenterol.* **21**(13), 3843–3849 (2015)
6. Ali, A., Plettenburg, D.H., Breedveld, P.: Steerable catheters in cardiology: classifying steerability and assessing future challenges. *IEEE Trans. Biomed. Eng.* **63**(4), 679–693 (2016)
7. Kim, Y., Parada, G.A., Liu, S., Zhao, X.: Ferromagnetic soft continuum ro-bots. *Sci. Robot.* **4**(33), eaax7329 (2019)
8. Gopesh, T., et al.: Soft robotic steerable microcatheter for the endo-vascular treatment of cerebral disorders. *Sci. Robot.* **6**(57), eabf0601 (2021)
9. Hu, X., Chen, A., Luo, Y., Zhang, C., Zhang, E.: Steerable catheters for minimally invasive surgery: a review and future directions. *Comput. Assist. Surg.* **23**(1), 21–41 (2018)

10. Soyama, T., Yoshida, D., Sakuhara, Y., Morita, R., Abo, D., Kudo, K.: The steerable micro-catheter: a new device for selective catheterisation. *Cardiovasc. Intervent. Radiol.* **40**(6), 947–952 (2017). <https://doi.org/10.1007/s00270-017-1579-3>
11. Sun, L., et al.: Biohybrid robotics with living cell actuation. *Chem. Soc. Rev.* **49**(12), 4043–4069 (2020)
12. Ricotti, L., et al.: Biohybrid actuators for robotics: a review of devices actuated by living cells. *Science Robotics* **2**(12), eaaq0495 (2017)
13. Hasebe, A., et al.: Biohybrid actuators based on skeletal muscle-powered microgrooved ultra-thin films consisting of poly (styrene-block-butadiene-block-styrene). *ACS Biomater. Sci. Eng.* **5**(11), 5734–5743 (2019)
14. Guix, M., et al.: Biohybrid soft robots with self-stimulating skeletons. *Sci. Robot.* **6**(53), eabe7577 (2021)
15. Pagan-Diaz, G.J., et al.: Simulation and fabrication of stronger, larger, and faster walking biohybrid machines. *Adv. Funct. Mater.* **28**(23), 1801145 (2018)
16. Regehr, K.J., et al.: Biological implications of polydimethylsiloxane-based microfluidic cell culture. *Lab Chip* **9**(15), 2132–2139 (2009)
17. Genchi, G.G., et al.: Bio/non-bio interfaces: a straightforward method for obtaining long term PDMS/muscle cell biohybrid constructs. *Colloids Surf. B* **105**, 144–151 (2013)
18. Park, S., et al.: Silicones for stretchable and durable soft devices: beyond sylgard-184. *ACS Appl. Mater. Interfaces* **10**(13), 11261–11268 (2018)
19. Sollier, E., Murray, C., Maoddi, P., Di Carlo, D.: Rapid prototyping polymers for microfluidic devices and high pressure injections. *Lab Chip* **11**(22), 3752–3765 (2011)
20. I. Mechanical Properties of Catheters. *Acta Radiol. Diagnosis* **4**, 11–22 (1966)
21. Huang, C., Bian, Z., Fang, C., Zhou, X., Song, J.: Experimental and theoretical study on mechanical properties of porous PDMS. *J. Appl. Mech. Trans. ASME* **85**(4), 041009 (2018)
22. Evans, R.L., Bernstein, E.F., Johnson, E., Reller, C., Mechancia, C.R.: Mechanical properties of the living dog aorta. *Am. J. Physiol.-Legacy Content* **202**(4), 619–621 (1962)
23. Bauchau, O.A., Craig, J.I.: Euler-Bernoulli beam theory. In: Bauchau, O.A., Craig, J.I. (eds.) *Structural analysis. Solid Mechanics and Its Applications*, vol. 163, pp. 173–221. Springer, Dordrecht (2009). [https://doi.org/10.1007/978-90-481-2516-6\\_5](https://doi.org/10.1007/978-90-481-2516-6_5)
24. Mestre, R., Patiño, T., Barceló, X., Anand, S., Pérez-Jiménez, A., Sánchez, S.: Force modulation and adaptability of 3D-bioprinted biological actuators based on skeletal muscle tissue. *Adv. Mater. Technol.* **4**(2), 1800631 (2019)
25. Hartquist, C.M., et al.: Quantification of the flexural rigidity of peripheral arterial endovascular catheters and sheaths. *J. Mech. Behav. Biomed. Mater.* **119**, 104459 (2021)
26. Basciano, C.A., Kleinstreuer, C., Kennedy, A.S., Dezarn, W.A., Childress, E.: Computer modeling of controlled microsphere release and targeting in a representative hepatic artery system. *Ann. Biomed. Eng.* **38**, 1862–1879 (2010)
27. Lai, S., Zucca, A., Cosseddu, P., Greco, F., Mattoli, V., Bonfiglio, A.: Ultra-conformable organic field-effect transistors and circuits for epidermal electronic applications. *Org. Electron.* **46**, 60–67 (2017)
28. Sakar, M.S., et al.: Formation and optogenetic control of engineered 3D skeletal muscle bioactuators. *Lab Chip* **12**(23), 4976–4985 (2012)
29. Vurro, V., et al.: Molecular design of amphiphilic plasma membrane-targeted azobenzenes for nongenetic optical stimulation. *Front. Mater.* **7**, 631567 (2021)

**Open Access** This chapter is licensed under the terms of the Creative Commons Attribution 4.0 International License (<http://creativecommons.org/licenses/by/4.0/>), which permits use, sharing, adaptation, distribution and reproduction in any medium or format, as long as you give appropriate credit to the original author(s) and the source, provide a link to the Creative Commons license and indicate if changes were made.

The images or other third party material in this chapter are included in the chapter's Creative Commons license, unless indicated otherwise in a credit line to the material. If material is not included in the chapter's Creative Commons license and your intended use is not permitted by statutory regulation or exceeds the permitted use, you will need to obtain permission directly from the copyright holder.

